ICAS 2016
30th Congress of the International Council of the Aeronautical Sciences
DCC, Daejeon, Korea ; September 25-30, 2016

NUMERICAL SIMULATION OF THE PROPELLER/WING INTERACTIONS AT LOW REYNOLDS NUMBER

Wang Hongbo*, Zhu Xiaoping, Zhou Zhou***
***School of Aeronautics, Northwestern Polytechnical University, Xi'an, China**
**** Science and Technology on UAV Laboratory, Northwestern Polytechnical University, Xi'an, China**

Keywords: *over airfoil propeller configuration, propeller slipstream, Propeller/wing interaction, negative drag, lift increment*

Abstract

The present investigation focuses on the propeller /wing interactions at a low Reynolds number flow. The objective is to research for a new aerodynamic configuration to increase lift force as well as lift-to-drag ratio and reduce drag force considerably. An over airfoil propeller configuration (OAPC) and two double airfoils coupled with a propeller configurations (DAPC and SDAPC) are investigated by using the ANSYS Fluent commercial software at a two dimensional flow. Steady Reynolds-Averaged Navier-Stokes (RANS) computations are conducted combining an actuator model to accurately simulate the propeller/wing aerodynamic interactions. The results reveal that these three new configurations can significantly reduce the drag even a minus value can be obtained due to a propeller slipstream, as a result, the conventional definition of lift-to-drag ratio is not suitable anymore for these new configurations. Although the overall aerodynamic performances for the DAPC and SDAPC configurations are debilitated slightly because of the unfavorable impact coming from the upper airfoil, these two arrangements are considered as good compromises during a wind range of flight from a small angle of attack to a high one. In addition, a heavy propeller disc load produces a beneficial effect on a decreasing drag coefficient and more potential can be exploited through a fully optimization.

1 Introduction

Environmental concerns and rising fuel consumptions in recent years have motivated increased research in solar powered aircrafts. In March 2015, a solar powered aircraft named Solar Impulse 2 began its journey around the world, which exhibits its outstanding ability of a zero-fuel-consumption flight.

Distributed electric propellers are often used for a high altitude and long endurance solar powered unmanned airplane with a high aspect ratio due to the low photoelectric conversion efficiency of a solar cell. As a result, a large part of the airplane's wing is immerged in the propeller slipstreams when many propellers rotate simultaneously such as the example of Helios prototype solar powered aircraft [1], whose propeller slipstreams cover more than 50% of the wing area. For a conventional tractor arrangement, a propeller slipstream can induce both the upwash and downwash effects [2-5] simultaneously, which change an aircraft's lift distributions apparently and make them more complicate. An unreasonable aerodynamic configuration design can cause unfavorable impacts on the aircraft's performance.

The purpose of this paper is to investigate a new configuration which can make advantage of the beneficial influence between the propeller and the wing to significantly improve the wing's performance and eliminate the disadvantages of the upwash and downwash effects. An over-the-wing propeller arrangement is one of the potential approaches to achieve this objective and experimental studies [6-10] have been conducted to prove this configuration. A

negative wing drag [11, 12] can also be obtained under some reasonable conditions. In this paper, the over-the-wing configuration as well as other two layouts based on it are studied by making use of the Computational Fluid Dynamics (CFD) method and two dimensional simulations are conducted to easily understand the reasons of the beneficial effects produced by these new configurations.

2 CFD Simulation Method

ANSYS Fluent software is used to simulate the interaction flow between a propeller and an airfoil at a low Reynolds number. For a two dimensional (2D) flow, the propeller geometry model is described by a straight line and its boundary condition can be implemented by an actuator disc model [13-15]. This model is a lumped parameter model which can be used to consider the influence of a propeller on an airfoil and it is necessary to for users to specify a pressure jump to simulate the propeller thrust. In addition, the k-k_L-ω turbulence model is selected for all computations in this paper, which is a transition model effectively predicting the transition of boundary layer from a laminar flow to a turbulent flow and has a higher accuracy during the low Reynolds number flow simulations.

3 Results and Discussion

3.1 Conventional Tractor Configuration

A conventional tractor propeller arrangement (Fig.1) is studied firstly for the purpose of showing aerodynamic forces of the airfoil immerging in a propeller slipstream. The airfoil is installed with an angle of 4 degrees and a free stream angle of attack of 2 degrees is selected in order to obtain the maximum lift-to-drag ratio at 6 degrees. The Reynolds number based the airfoil chord is $Re = 4.88\times10^5$ and the propeller diameter is 1.65m with a constant thrust T=23.2N corresponding to a design rotation speed 1500r/min.

As presented in Table.1, the presence of a propeller slipstream induces both increments in airfoil lift and drag coefficients at propeller positions $\Delta Y/R = -0.5$ and $\Delta Y/R = 0$ (R represents the propeller radius). A good effect of increasing lift and reducing drag, however, can be obtained when the propeller rotation axis is located higher than the airfoil chord plane.

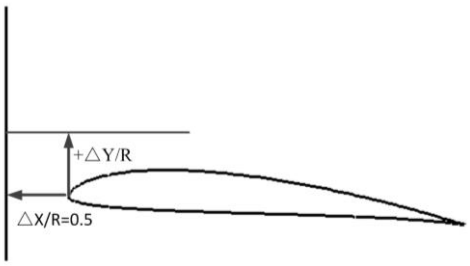

Fig.1 conventional tractor propeller configuration

Table.1 aerodynamic coefficients of tractor propeller layout

	C_l	C_d	C_m
Single airfoil	1.1187	0.01071	-0.09232
$\Delta Y/R = -0.5$	1.2491	0.02570	-0.10254
$\Delta Y/R = 0$	1.3053	0.01886	-0.110833
$\Delta Y/R = 0.5$	1.3173	0.008793	-0.107105

3.2 Over Airfoil Propeller Configuration

The favorable effect for a higher propeller position has shown the possibility of promoting airfoil performance affected by a propeller slipstream. Based on this conclusion, an over airfoil propeller configuration (Fig. **2**) is investigated to demonstrate the potential capability of considerably increasing airfoil lift and reducing airfoil drag for this arrangement.

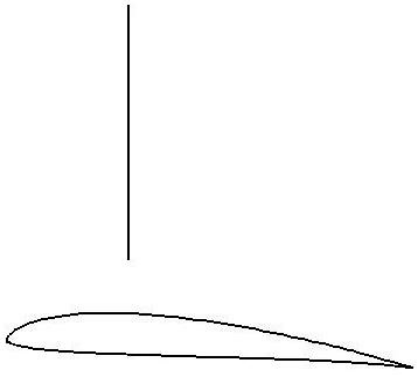

Fig. 2 over airfoil propeller configuration (OAPC)

The simulation results versus propeller streamwise installed positions are presented in Fig.3 for three propeller clearance values of

$\Delta Y/c = 0.1,\ 0.2,\ 0.3$ (c represents the airfoil chord) and the propeller disk plane is perpendicular to the freestream direction.

As expected, there is a considerable lift increment and a drag decrement for the over airfoil propeller configuration (denoted OAPC). Really exciting is that the airfoil drag can be reduced to a minus value that means a pushing force can be generated on the airfoil at this arrangement.

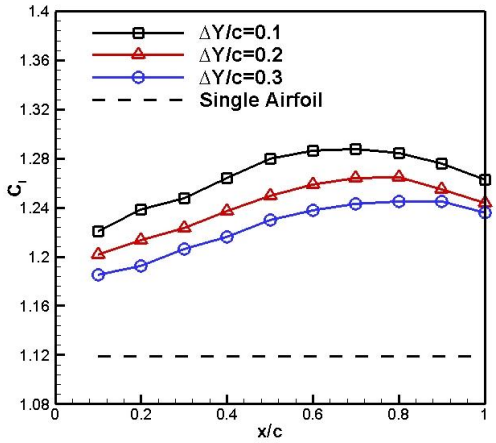

a) lift coefficients

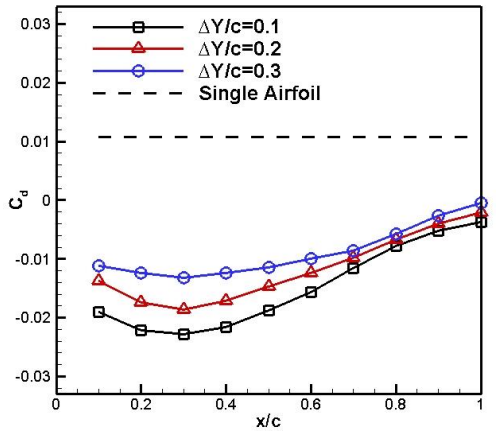

b) drag coefficients

Fig.3 Effect of propeller streamwise position on the OPAC

Significant gains in the airfoil lift and drag are experienced when moving the propeller backward. As a result, the maximum lift appears at the streamwise positon x/c=0.8 but the minimum drag is at x/c=0.3. In addition, the propeller clearance distance from the airfoil upper surface also shows an important impact on the behavior of the airfoil performance. A smaller clearance is favorable for enhancing lift and reducing drag. In the case of $\Delta Y/c = 0.1$, the lift coefficient can be increased by 11.5% at x/c=0.3 and 14.8% at x/c=0.8 (Table.2). However, the magnitude of drag decrement can unexpectedly achieve 313% and 173% respectively. Because of the negative drag value, it should be pointed out that the conventional definition of lift to drag is not suitable anymore for this unconventional configuration.

Table.2 comparisons of airfoil aerodynamic coefficients

Configuration	C_l	C_d	C_m
Single airfoil	1.1187	0.01071	-0.09232
OAPC(x/c=0.3)	1.2478	-0.02279	-0.08231
OAPC(x/c=0.8)	1.2847	-0.007816	-0.09602

Comparing the conventional propeller tractor arrangement, the OAPC configuration exhibits a excited advantage in the goal of increasing lift and decreasing drag. The reason for this beneficial phenomenon can be explained by the suction effect on the upper surface of the airfoil induced by the propeller (Fig.4). When the propeller is located over the airfoil, the axial free stream velocity is augmented by the propeller slipstream acceleration effect and the static pressure is decreased, as a result, the leading-edge suction fore of the airfoil will be enhanced correspondingly. It is the leading-edge suction force that causes a minus drag coefficient and pull the airfoil forward, which is also the reason why the minimum drag appears approximately the leading edge of the airfoil.

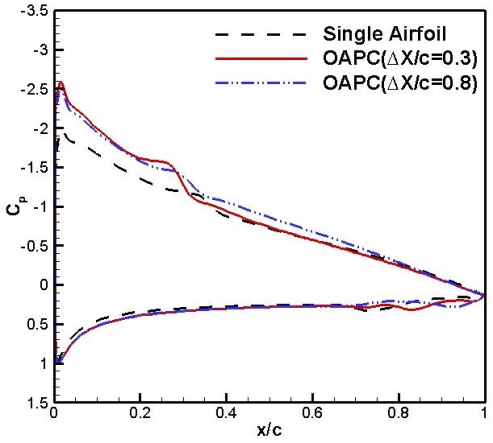

Fig.4 comparisons of pressure distributions on the OPAC configuration

3.3 Double Airfoils Propeller Configuration

According to the results of OAPC configuration, the mutual interaction between the propeller and the airfoil has the probability of producing a beneficial influence on the airfoil aerodynamic performance when the propeller locates at a reasonable position.

In this section, another new configuration (denoted DAPC) (Fig. 5) is investigated for the purpose of researching the airfoil aerodynamic behaviors under the mutual influence between two airfoils and a propeller. The distance between these two airfoils is equal to the airfoil chord. The propeller clearance is selected as the value $\Delta Y / c = 0.1$ and its streamwise position is selected as x/c=0.3 due to the minimum drag at this position.

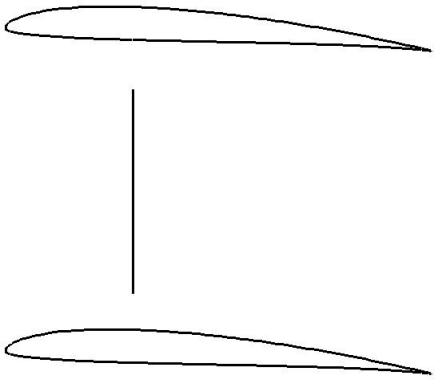

Fig. 5 double airfoils propeller configuration (DAPC)

As shown in Table.3 the mutual interaction between two airfoils causes frustrating overall performances compared with those at the OAPC configuration. It is obvious that the presence of an upper airfoil induces decrements in lift but increments in drag for these two airfoils. Although the lift-to-drag ratio for the DAPC configuration is smaller than that of the OAPC arrangement, it is nearly 12 times higher than that of the single airfoil according to the conventional definition of lift-to-drag ratio.

Table.3 airfoil aerodynamic coefficients at DAPC configuration

		Cl	Cd
Single airfoil		1.1187	0.01071
DAPC	Upper airfoil	0.4614	0.011757
	Lower airfoil	0.5329	-0.010968
	Total	0.9943	0.0007894

The impact of the mutual interaction between these two airfoils can be demonstrated by the pressure distributions in Fig.6. For the upper airfoil (Fig.6a), the region affected by the propeller suction effect mainly focuses on the lower surface of the upper airfoil where the lower static pressure happens due to the increasing axial free stream velocity, as a consequence, the pressure difference distributed on the upper airfoil is decreased that represents a decreased lift. For the lower airfoil (Fig.6b), the influence induced by the propeller on it is the same as that of the OAPC configuration but the pressure difference acting on the lower airfoil is still smaller than that of the single airfoil, which also means a decreased lift. Apart from this, the reflection effect that the higher pressure coming from the upper airfoil's lower surface acting on the upper surface of the lower airfoil is another reason of reducing the lower airfoil's performance. (see Fig.7)

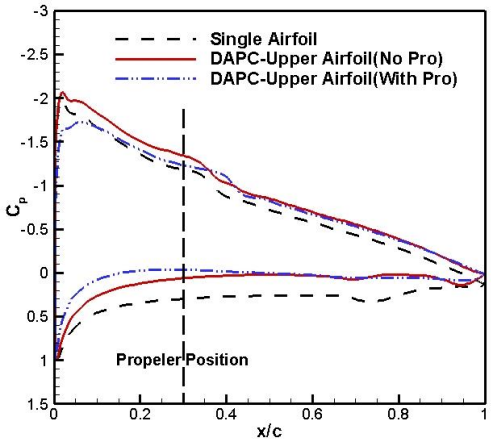

a) pressure contributions of the upper airfoil

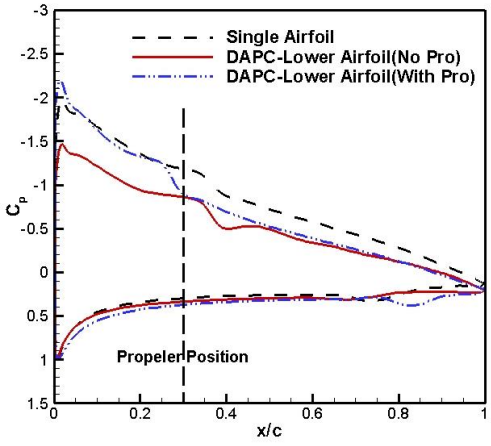

b) pressure contributions of the lower airfoil

Fig.6 chordwise pressure distributions for the DAPC configuration

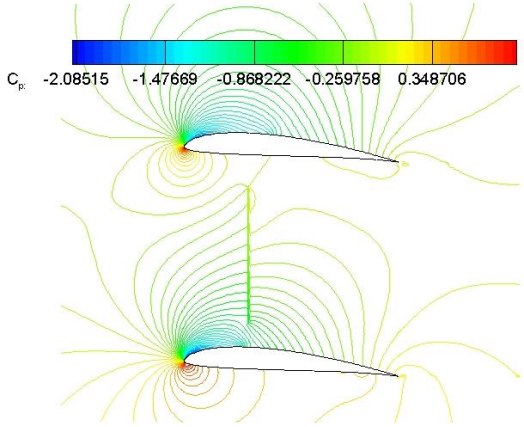

Fig.7 pressure contours of the DAPC configuration

3.4 Scaled Double Airfoil Propeller Configuration

The forementioned calculated results in section 3.3 indicate that the presence of the upper airfoil will cause an unfavorable influence on the overall performance for the DAPC configuration. In order to overcome the disadvantage of this arrangement, a third new configuration denoted as SDAPC is investigated. For this layout, the upper airfoil chord is scaled down to 40% of the original length and the propeller position is moved backward to the value of x/c=0.8 (Fig.8).

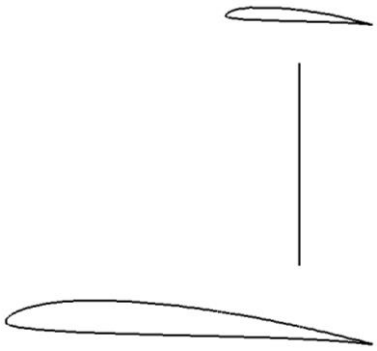

Fig.8 scaled double airfoils propeller configuration (SDAPC)

Comparing with the DAPC configuration, the lift coefficients shown in Table.4 present a 9.6% increment and the lift-to-drag ratio is almost 4 times higher than that of the single airfoil. Judging from the overall performance, it is noticeable that this SDAPC configuration is a compromise one between the OAPC and the DAPC configurations.

Table.4 airfoil aerodynamic coefficients at the SDAPC configuration

		Cl	Cd
Single airfoil		1.1187	0.01071
SDAPC	Up airfoil	0.20237	0.01434
	Down airfoil	0.88749	-0.01167
	Total	1.0899	0.00267

Fig.9 describes pressure distributions of the SDAPC configuration. The smaller lift coefficient of the upper airfoil can still be attributed to the lower pressure distributed on its lower surface (Fig.9a). As for the lower airfoil (Fig.9b), the leading-edge suction force plays an important role in lift augment and drag reduction. Furthermore, the unfavorable impact of the reflection effect coming from the upper airfoil is weaken due to the smaller chord of the upper airfoil (Fig.10).

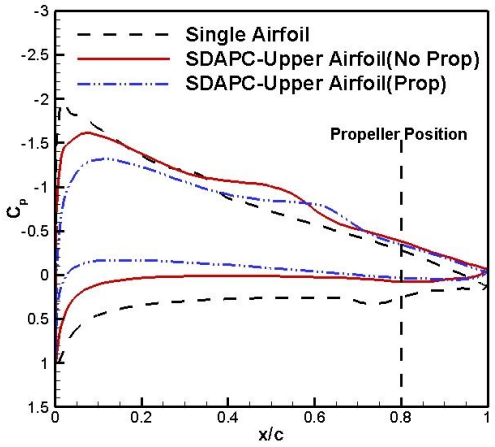

a) pressure distributions of the upper airfoil

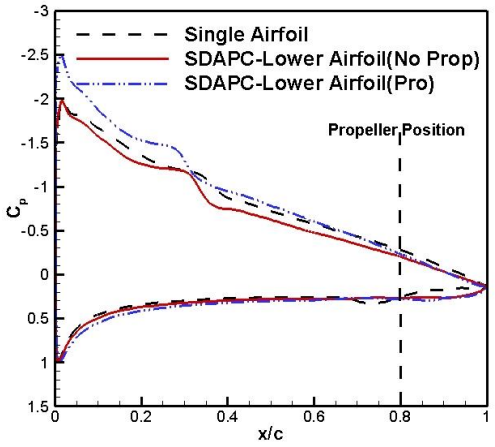

b) pressure distributions of the lower airfoil

Fig.9 chordwise pressure distributions of the SDAPC configuration

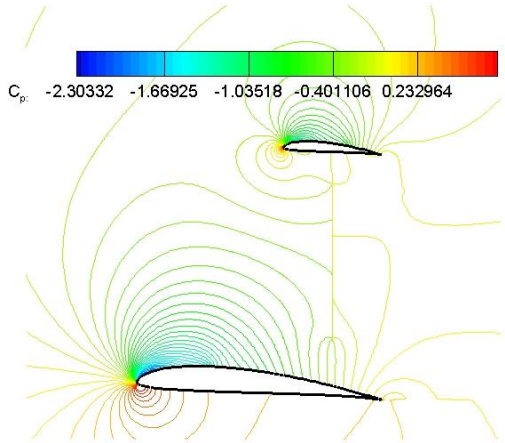

Fig.10 pressure contours of the SDAPC configuration

3.5 Propeller Diameter Effect

Besides the aerodynamic configuration investigation, the propeller diameter effect on the DAPC and SDAPC configurations is investigated in this section. The variation range of the propeller diameter (denoted D) is selected from 0.2 to 1.0 and the propeller thrust is kept as a constant value when its diameter changes.

The results plotted in Fig.11 demonstrate that a smaller propeller diameter produces a slight lift increment but a considerable drag reduction especially for the DAPC configuration. This phenomenon can be explained by the effect of the combination of the suction effect at the leading edge and a pushing effect at the rear edge of the lower airfoil when the propeller diameter is reduced to be a small value.

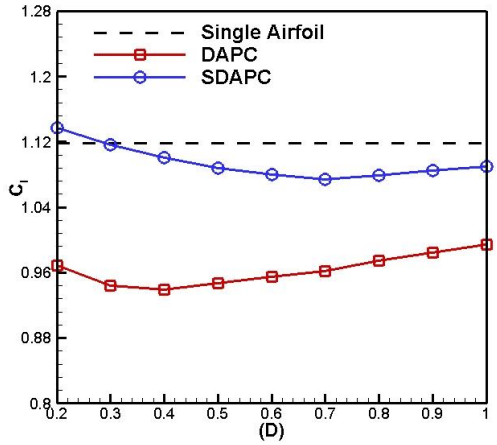

a) lift coefficients

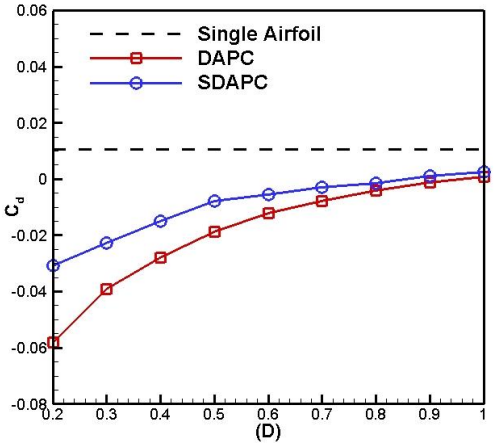

b) drag coefficients

Fig.11 propeller diameter effects on different configurations

3.6 Propeller Thrust Effect

In this section, another propeller parameter, the propeller thrust, is also studied for the DAPC and SDAPC configurations. The variation range of the thrust is selected from 10N to 130N (Fig.12) and the propeller diameter is kept as a constant value.

Apparently, an increasing propeller thrust induces an increasing lift force and a decreasing drag force. In the case of a constant diameter, a higher propeller thrust means a higher disc load, hence, a stronger suction effect at the airfoil leading edge and a pushing effect behind the propeller disc plane both make contributions to considerably improve the aerodynamic performances of these two configurations.

For a low speed and incompressible flow, the increasing free stream velocity leads to a lower static pressure in front of the propeller disc plane according to Bernouilli's principle, which is the root cause of the leading-edge suction effect. In addition, both the static and total pressure are increased after the propeller disc plane, which produce a pushing effect on the rear segment of the airfoil. As a result, it is the combination of the suction effect on the airfoil leading edge and the pushing effect on the airfoil rear edge that reduce the airfoil drag to be a smaller even a minus value.

Based on the calculated results, the SDAPC configuration has an advantage over the DAPC configuration in the ability of enhancing lift coefficient and reducing drag coefficient.

Moreover, a higher propeller disc load is more beneficial for the airfoil aerodynamics.

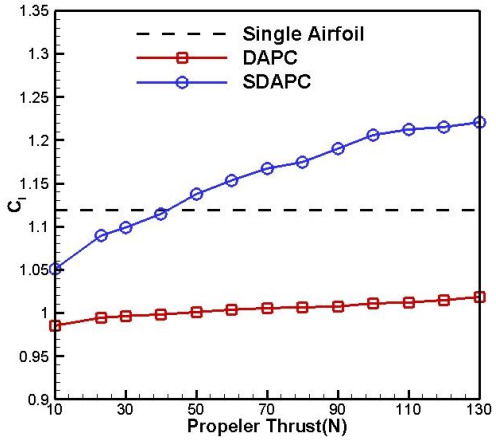

a) lift coefficients versus the propeller thrust

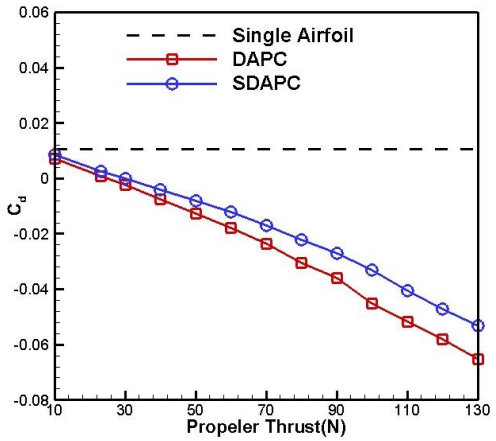

b) drag coefficients versus the propeller thrust

Fig.12 propeller thrust effect on different configurations

3.7 Large angle of attack effect

In order to show the advantages of the DAPC and SDAPC configurations, the effect of large angles of attack is presented in Fig.13. Although the lift coefficients for these two configurations are smaller than those of the single airfoil and the OAPC configurations, the drag coefficients are also much smaller especially at high angles of attack. Therefore, the advantages of smaller drag for these two arrangements also can be obtained for a high angle of attack flight.

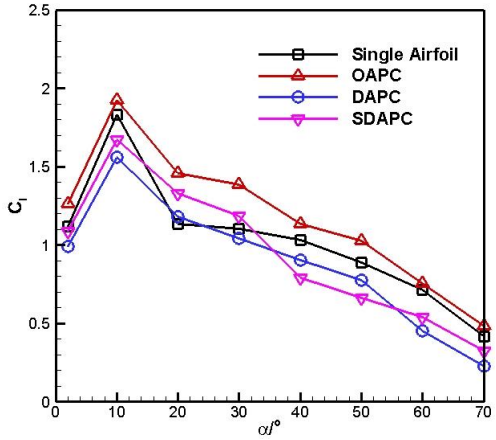

a) lift coefficients versus angles of attack

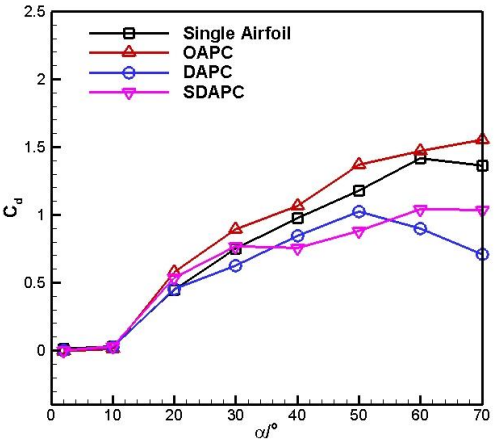

b) drag coefficients versus angles of attack

Fig.13 effect of angles of attack on different configurations

3.8 Ground effect

Considering the excellent flight ability at a wide range of angle of attack for DAPC and SDAPC configurations, the ground effect is studied in this section to obtain the further potential. A zero free stream velocity at the standard atmosphere condition is selected to conduct the numerical simulations.

As can be seen in Table.5, the aerodynamic forces are different for each other. Except the propeller thrust, the upper and lower airfoils of the DAPC configuration both generate lifts in spite of a small magnitude, which is caused by the beneficial suction effect (Fig.14a) at the leading edge of the airfoil. For the SDAPC configuration, a suckdown effect (Fig.14b) is induced by the large separation area at the rear segment of the lower airfoil, which leads to a small magnitude of lift even a negative lift, as a

result, the total lift for this configuration is almost zero.

It is obvious that the DAPC arrangement has the advantage of generating lifts to reduce the engine power at the vertical take-off and landing (VTOL) phases for a VTOL aircraft. Therefore, this configuration seems to be a potential layout for the VTOL aircraft design in the future, of course, it needs more detailed three dimensional simulations and a fully optimization.

Table.5 comparisons of lifts with ground effects

Configuration	Upper airfoil	Lower airfoil	Total
DAPC	7.61	5.72	13.33
SDAPC	1.28	-0.38	0.90

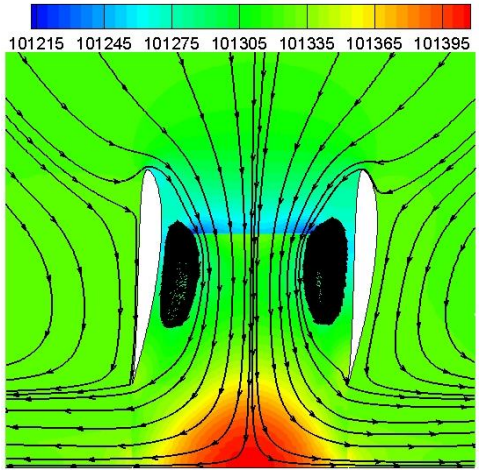

a) DAPC configuration

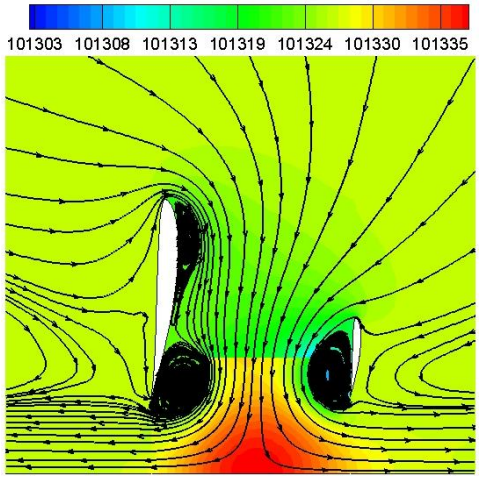

b) SDAPC configuration

Fig.14 pressure contour distributions with the ground effect

4 Conclusions

For the purpose of making advantage of a propeller slipstream to obtain beneficial effects on an airfoil aerodynamic performance, numerical simulations using ANSYS Fluent software are conducted at a low Reynolds number 2D flow. A single airfoil, an over-airfoil-propeller configuration and two types of double airfoils coupled with a propeller configuration are compared at different propeller positions and with different diameters as well as thrusts. An assessment of these three configurations reveals that all of them have an advantage of enhancing lift coefficient and reducing drag coefficient considerably. A minus drag coefficient can be obtained for these configurations, as a result, the conventional definition of lift-to-drag ratio is not suitable anymore for these new configurations.

Because of the beneficial influence of the propeller, the negative drag fore is generated by the combination of the suction effect at the leading edge and the pushing effect at the rear edge of the airfoil. For the DAPC and SDAPC configurations, the reflection effect of the upper airfoil on the lower airfoil leads to an unfavorable impact on the overall aerodynamic performances. However, both of these two configurations show the better characteristics at high angles of attack flight. For this reason, they are considered as good compromises for the flight ability at a wide range of angle of attack. Apart from this, a higher propeller disc load is favorable for the aerodynamic forces of the airfoil especially for the ability of reducing the drag due to the stronger suction and pushing effects.

The aforementioned new configurations may exploit more aerodynamic potentials through a fully optimization. Further efforts should be extend to the studies of the propeller characteristics and a three dimensional flow simulation because of the more complicate problems for a 3D configuration.

References

[1] Noll T E, Ishmael S D, Henwood B, et al. Technical findings, lessons learned and recommendations resulting from the helio prototye vehicle mishap[R],

National Aeronautics and Space Admin Langley Research Center Hampton VA, 2007.
[2] Ferraro G, Kipouros T, Savill A M, et al.Propeller-Wing interaction prediction for early design[C]// AIAA SciTech: Science and Technology Forum and Exposition, National Harbor, Maryland. 2014.
[3] ILAN K. Propeller-Wing integrations for minimum induced loss[J]. Journal of Aircraft, 1986, 23(7): 561-565.
[4] QIN E, YANG Guowei, LI Fengwei. Numerical analysis of the interference effect of propeller slipstream on aircraft flowfield[J]. Journal of Aircraft, 35(1): 84-90.
[5] WITKOWSKI D P, ALEX K L, SULLIVAN J P. Aerodynamic interaction between propellers and wings[J]. Journal of Aircraft, 1989, 26(9): 829-836.
[6] PUTNAM L. Exploratory investigation at Mach numbers from 0.4 to 0.95 of the effect of jets blown above a wing[R], NASA TN D-7367, 1973.
[7] SAWYER R A, MECALFE M P. Jet/Wing interference for an overwing engine configuration[R], AGARD CP-285, 1980.
[8] JOHNSON J L, WHITE E R. Exploratory low speed wind-tunnel investigation of advanced commuter configurations, including an over-the-wing propeller[R], AIAA-83-2531, 1983.
[9] LLM Veldhuis. Experimental analysis of tractor propeller effects on a low aspect ratio Semi-Span wing[C]//Second Pacific International Conference on Aerospace and Technology, 1995: 491-498.
[10] LUIJENDIJK A M. Propeller-wing interference study for over the wing positioned propeller configurations[D]. Delft: Delft University of Technology, 2002.
[11] LLM Veldhuis. Propeller wing aerodynamic interference[D]. Delft: Delft University of Technology, 2005.
[12] MÜLLER L, HEINZE W, DRAGAN K. Aerodynamic installation effects of an Over-the-Wing propeller on a High-Lift configuration[J]. Journal of Aircraft, 2014, 51(1): 249-258.
[13] THOUAULT N, BREITSAMTER C, GOLOGAN C, et al. Numerical analysis of design parameters for a generic fan-in-wing configuration[J]. Aerospace Science and Technology, 2010, 14(1): 65-77.
[14] FARRAR B, AGARWAL R. CFD analysis of open rotor engines using an actuator disk model[C]//52nd AIAA Aerospace Sciences Meeting, 2014: 0408-2014.
[15] VELDHUIS L M, LUURSEMA G W. Comparison of an actuator disk and a blade modeling approach in Navier-Stokes calculations on the SR-3[C]//Fluid Dynamics and Co-located Conferences. America, 2000: 924-932.

Contact Author Email Address

whb0126@163.com

Copyright Statement